Flip Angle Inhomogeneity Constrained pTx Pulse Design for Minimum Peak Local SAR

Mihir Pendse[1], Simone Winkler[2], and Brian Rutt[2]

[1]*Department of Electrical Engineering, Stanford University, Stanford, CA, United States,* [2]*Department of Radiology, Stanford University, CA, United States*

Target Audience: Researchers and engineers interested in RF safety and parallel transmit

Purpose: A major concern in parallel transmission (pTx), especially at high static field strengths, is the risk of exceeding peak local SAR (pkSAR) regulatory limits due to the nontrivial relationship between transmitted power and local SAR in multichannel excitation. pTx SAR patterns are pulse dependent requiring the computation of SAR matrices from *E*-field maps simulated using patient-matched body models. The expectation is that actual patient B_1+ maps, along with the SAR matrices, will be used for real-time pTx pulse design. One of the first notable works to incorporate SAR into spokes-based pTx pulse optimization[1] cast the problem as a minimization of flip angle inhomogeneity (FAI) subject to an absolute pkSAR constraint (*P*) [see †]. The main drawback of this "constrSAR" method is that determining the optimal pulse for a specified FAI threshold requires one to perform several optimizations with different SAR constraints. Here we reformulate the problem by minimizing pkSAR subject to a FAI constraint (*F*) [see ‡] and demonstrate superior performance of this "minSAR" method for many realistic situations in addition to the direct benefit of specifying *F* up front.

† **constrSAR:**	‡ **minSAR:**
MINIMIZE: FAI	MINIMIZE: $pkSAR$
SUBJECT TO:	SUBJECT TO:
$pkSAR \leq P$	$FAI \leq F$

Theory: The local SAR at a given voxel can be computed as $\mathrm{SAR}(\mathbf{x}) = \mathbf{b}^{\mathrm{H}}\mathbf{Q}(\mathbf{x})\mathbf{b}$ where $\mathbf{b}$ is the unitless complex RF pulse amplitude at each coil element, and $\mathbf{Q}(\mathbf{x})$ is the local SAR matrix, a positive semi-definite Hermitian matrix that incorporates *E*-fields and tissue properties. For computational tractability, the SAR matrices are typically compressed using Virtual Observation Points [2] yielding a reduced set of *M* matrices $\{\mathbf{A}_1,..,\mathbf{A}_M\}$ such that $\max(\mathbf{b}^{\mathrm{H}}\mathbf{A}_1(\mathbf{x})\mathbf{b},\ldots,\mathbf{b}^{\mathrm{H}}\mathbf{A}_M(\mathbf{x})\mathbf{b})$ estimates pkSAR with no underestimation and bounded overestimation. Using this compressed set of matrices, the optimum pulse $\tilde{\mathbf{b}}$ can be computed through ‡ which is a convex optimization since $\mathrm{pkSAR} = \|[\tilde{\mathbf{b}}^{\mathrm{H}}\tilde{\mathbf{A}}_1\tilde{\mathbf{b}} \quad \cdots \quad \tilde{\mathbf{b}}^{\mathrm{H}}\tilde{\mathbf{A}}_M\tilde{\mathbf{b}}]\|_\infty$ and $\mathrm{FAI} = \|\mathbf{E}\tilde{\mathbf{b}} - \mathbf{d}\|_2 / \|\mathbf{d}\|_2$ where $\tilde{\mathbf{b}}$ is the pulse on each coil element for each spoke, $\mathbf{E}$ is the system matrix [3], and $\mathbf{d}$ is the complex transverse magnetization at all voxels of interest. Since the system matrix $\mathbf{E}$ is a function of spokes locations ($\mathbf{k} = [k_x, k_y]$), updating $\mathbf{k}$ to reduce FAI (at fixed $\tilde{\mathbf{b}}$) can expand the range of pulses that satisfy the FAI constraint so pkSAR decreases when optimized at the updated location. Thus a desirable framework for the pulse design is a two-step iterative method: optimization of $\tilde{\mathbf{b}}$ at fixed $\mathbf{k}$ interleaved with optimization of $\mathbf{k}$ at fixed $\tilde{\mathbf{b}}$.

Table 1	Case 1	Case 2	Case 3	Case 4
Stopping Criteria	change in objective $< 0.1\%$	one minute comp. time	single iteration	one minute comp. time
SAR Matrix Accuracy	High	High	High	Low

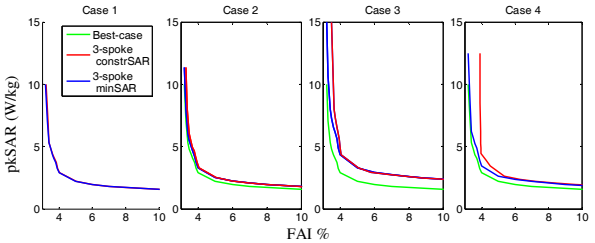

Fig. 1: L-curves for each case described in Table 1

Methods: SAR matrices at each voxel were computed using *E*-field maps generated through FDTD simulations with SEMCAD X (SPEAG, Zurich, Switzerland) and the Ella body model (Virtual Family, IT'IS, Zurich, Switzerland), using an 8-element head-sized loop array operating at 298 MHz (7T). To assess the sensitivity of the optimization to errors in the estimated *E*-fields, a second set of SAR matrices was computed from a simulation with a coarser FDTD grid. Both datasets were compressed, resulting in 835 matrices with a mean pkSAR overestimation of 2.65% for the fine grid and 543 matrices with a mean overestimation of 53.2% for the coarse grid. To implement the nonconvex optimization of $\mathbf{k}$, we used the computationally efficient method of minimizing parabolic surrogates for the FAI expression [4]. Although compressed data sets were used for all pulse optimizations, true pkSAR was computed by an exhaustive search over all SAR matrices from the finer FDTD grid. A duty cycle of 10% and a target flip angle of 45 degrees were used to compute absolute SAR values (in W/kg). The pTx subpulse duration was adjusted based on number of spokes so that total pulse duration was always 4 ms. The target phase of the excitation was chosen based on MLS target phase [1] and was updated at each iteration. To initialize the optimization, regularized least squares with a penalty on pulse power was used to minimize FAI with spokes location updates (if needed) until FAI was below the specified threshold (Fig. 3). Both the proposed minSAR and original constrSAR method were implemented to produce L-curves for the cases in Table 1. Case 1 represents the ideal L-curve using accurate SAR matrices and a conservative stopping condition. Case 2 and Case 3 also use the accurate SAR matrices but limit the duration of the computation to either one minute (Case 2) or one iteration (Case 3). Case 4 is meant to most resemble the situation of an actual scan where computation time is limited and SAR matrices also have some error (due to both patient / body model mismatch and compression).

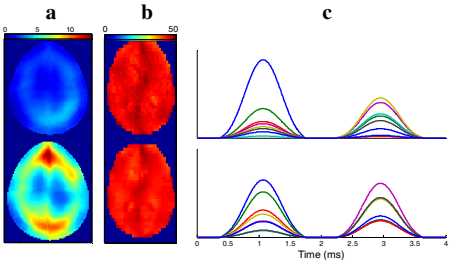

Fig. 2: **(a)** SAR maps of slice with peak local SAR in W/kg, **(b)** flip angle maps in degrees, and **(c)** relative magnitude of pulse across all channels for minSAR optimization (top row, FAI = 5.10) and constrSAR optimization (bottom row, FAI = 5.08) using 2-spoke 4ms pulse with conditions in Case 4.

Results: As seen in Fig. 1, the minSAR and constrSAR formulations are nearly identical for Case 1 and 2 but for Case 3 and 4, the minSAR curve is clearly seen to be to the left of the constrSAR curve for FAI values below about 5%. A similar result is seen in Fig. 2 where the minSAR 2-spoke pulse achieves a substantially lower SAR map than the constrSAR pulse despite nearly identical FAI. The deviation of the L-curves in Case 2 and 3 from the best case is understood by observing Fig. 3 and noting that although pkSAR reduces significantly in just one iteration, as spokes locations are updated there is a slow but steady reduction in pkSAR.

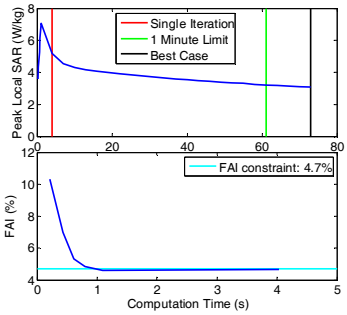

Fig. 3: Progression of the optimization

Discussion and Conclusion: For all cases tested, the minSAR approach achieves equal or lower SAR values than the constrSAR method for low values of FAI. The two approaches differ for the following fundamental reason: due to overestimation of SAR from the compression, the SAR constraint in the constrSAR method is overly strict so FAI is being minimized over only a subset of all pulses that truly meet the SAR constraint, resulting in a larger minimum FAI. With the minSAR method, the set of pulses that meet the FAI constraint is constant and insensitive to errors in SAR estimation. Although the minimization over this set is done with overestimated SAR values, the positive bias is corrected when the true SAR is recomputed using the full, accurate SAR matrix dataset. This fundamental benefit is amplified when computation time is limited or when SAR estimation has significant error, both of which are situations that should be expected in an actual scan. The proposed minimum SAR pTx pulse design introduced here allows one to directly specify a target FAI and obtain a minimum pkSAR pulse with more robustness to real-world limitations than the constrained SAR method.

References: [1] Guerin, et. al, MRM 2013, [2] Eichfelder MRM 66:1468-1476 (2011), [3] Grissom MRM 56:620-629 (2006) [4] Grissom MRM 68: 1553-1562 (2012)